

# A Low Power Read-out Sensor for Detecting Harmful Gas

Joo Hwan Jin<sup>1</sup>, Seung Jun Lee, Ki Hyun Kim, Ju Yong Lee and Hyung Il Chae<sup>a</sup>

Department of Electrical Engineering, Konkuk University

E-mail : <sup>1</sup>ajdddj789@konkuk.or.kr

**Abstract** - Interest in air quality is increasing due to the awareness of the seriousness of air pollution, resulting in continuous monitoring of harmful ingredients in the air. Sensors incorporating Internet of Things (IoT) capabilities are required to efficiently collect general user and atmospheric environment information in a wide range. Therefore, it is necessary to develop low-cost, ultra-small, and low-power sensors to install a large number of sensors in a wide range. In this paper, Read-Out Integrated Circuit (ROIC) is proposed to aim to develop low-cost, ultra-small, low-power, and high-sensitivity sensors based on High-Electron Mobility Transistors (HEMT) incorporating IoT functions with semiconductor-type gas sensors. The proposed ROIC utilizes Transimpedance Amplifier (TIA), Delta-Sigma Analog-to-Digital Converter (ADC), and Negative Charge Pump (NCP) in the TSMC 0.18um process.

**Keywords**—Delta-sigma ADC ( $\Delta\Sigma$  ADC), Gas sensor, HEMT device, Negative Charge Pump (NCP), Read-Out Integrated Circuit (ROIC), Transimpedance Amplifier (TIA)

## I. INTRODUCTION

Due to the recent inflow of fine dust, it is necessary to check the components of fine dust and prepare accordingly. Developed countries such as the United States, Australia, Japan, etc. are preparing specific standards for air pollutants and conducting systematic management, and prepare standards for carbon monoxide, lead, sulfur dioxide, and nitrogen dioxide by analyzing pollutants and collecting information on human hazards. Demand for harmful gas detection is soaring, but existing gas detection sensors are developed for special spaces such as factories and are large and are not subject to the public at a high cost. Sensors that incorporate IoT functions are needed to efficiently collect general atmospheric environment information. To install a large number of sensors in a wide range, the development of low-power, low-cost, and ultra-small sensors are needed. Commercialized electrochemical gas sensors have simple operation and high sensitivity, but they are inappropriate for home use and have limitations in miniaturization as they contain chemicals in the sensors. In this paper, we propose the development of a HEMT element-based sensor, which

a. Corresponding author; hichae@konkuk.ac.kr

Manuscript Received Oct. 22, 2021, Revised Nov. 29, 2021, Accepted Nov. 30, 2021

This is an Open Access article distributed under the terms of the Creative Commons Attribution Non-Commercial License (<http://creativecommons.org/licenses/by-nc/3.0>) which permits unrestricted non-commercial use, distribution, and reproduction in any medium, provided the original work is properly cited.

combines IoT function with semiconductor gas sensor. The HEMT device is a sensor that sensitively responds to changes in electrons on the surface, and changes into a current signal when gas is detected at the gate[1]. The characteristic curve shown in Figure 1 is shown, and it can be seen that the highest sensitivity is obtained when a negative voltage is applied. Figure. 2 shows the proposed ROIC's block diagram. HEMT device gate biasing is formed by negative voltage. Therefore, using the proposed NCP structure, create a negative voltage at the gate [2]. If harmful gases are formed on HEMT devices, the current changes as the Threshold Voltage of the HEMT element changes. The corresponding current signal is amplified to voltage using TIA to convert the analog signal into a digital signal with  $\Delta\Sigma$  ADC [3] – [7].

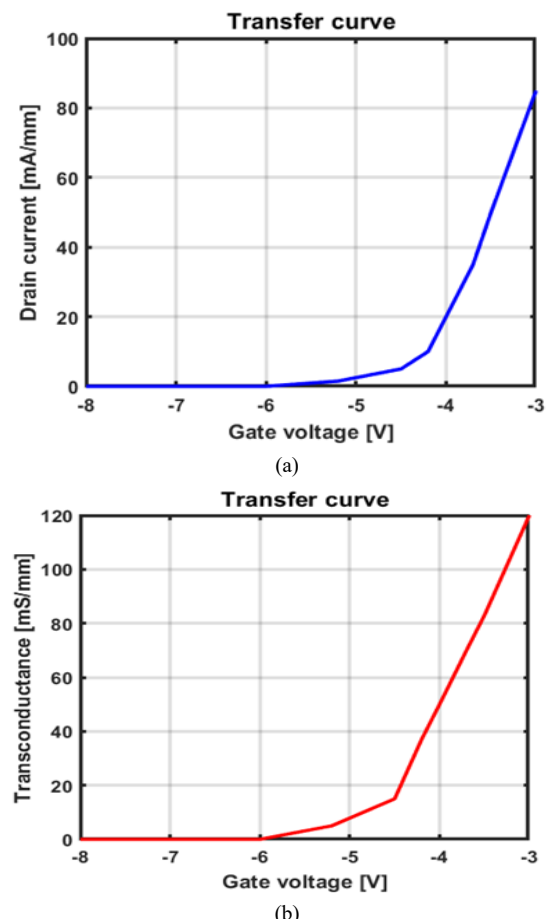


Fig. 1. (a) Drain current and (b) transconductance transfer curve of HEMT element.

## II. PROPOSED ARCHITECTURE AND IMPLEMENTATIONS

### A. Negative Charge Pump

As in Fig. 2, the HEMT element changes the drain current and transmission by the negative gate voltage. Increase detection sensitivity by setting the gate voltage that changes most sensitively when the threshold changes due to the formation of hazardous gas on the HEMT element. Therefore, an NCP consisting of Fig. 3 is proposed to output voltage in the range -7V to -2V. The proposed NCP consists of a total of two tiers, each of which is designed with a conventional double-based negative charge pump as shown in Fig. 4[2]. The clocks supplied to the NCP act as the control of the output voltage and are generated by a total of six 6-stage inverter chains. The size of the Clock is determined by the voltage supplied to the Low-dropout regulator (LDO) and the output voltage of the LDO is determined through a 16-step register reader, such as Fig. 5.

### B. Trans-impedance Amplifier

When various harmful gases present in nature are detected using the Negative Charge Pump and HEMT elements, the detected signal is small in size and cannot be processed directly through the Analog to Digital Converter. Therefore, a process of sufficiently amplifying the change in these small signals is needed, which is used at this time. At this time, attenuation and elimination of noise and offset during the process of amplifying the signal is essential. For this reason,

if noise and offset are not attenuated, noise and offset are amplified together during the amplification process of small signals, making it a big problem for signal detection. For this purpose, a nested coper structure was used where two low and high frequency choppers were placed at the input and output ends of the TIA, as shown in Fig. 6[3].

When using a common chopper, there is a problem with generating DC offsets in the high frequency band. However, when using a nested-chopper structure, as shown in Fig. 6, both the noise and signal are sent to the high frequency band through the chopper at the input level and amplified through the amplifier [4]. After that, bringing the signal back into the low frequency band can solve the problems of the existing chopper as it can produce the required noise performance. The changing drain current of the HEMT varies greatly from about 10uA to 1 mA. Therefore, the TIA's feedback resistance should also be set to be sufficiently amplified within this range. For this purpose, a total of four cases, 1k, 5k, 50k, and 200k, were divided into the two-bit decoder to allow control by digital. This enables the response and amplification of detection by the drain current of the HEMT element up to 1uA to 1 mA. Because this ROIC is aimed at low power, the TIA's design must also effectively amplify small signals while using low power. Therefore, the amplifier consists of a total of 2-stage. The first stage consisted of a component input amplifier, as shown in Fig. 7. In the case of conventional differential amplifiers, they have the advantage of being simple to design, but by not using the PMOS as input, but as a role to hold common-

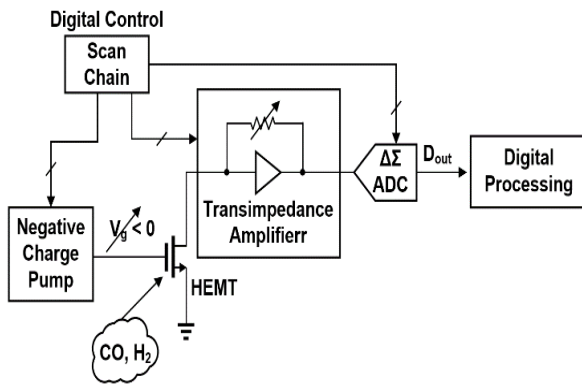


Fig. 2. The proposed ROIC's block diagram.

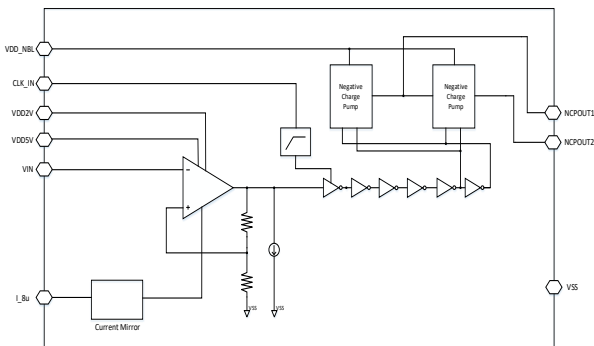


Fig. 3. The proposed Negative Charge Pump Block Diagram.

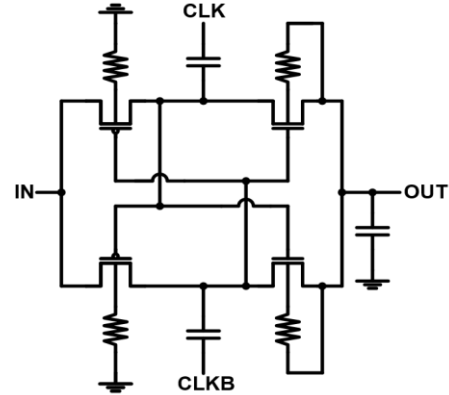


Fig. 4. Two stage conventional doubler-based negative charge pump.

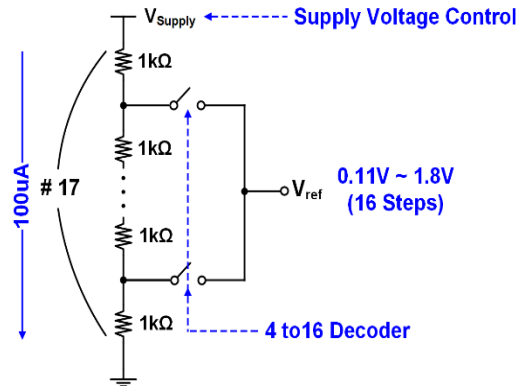


Fig. 5. 4-bit Resistor Ladder.

mode, they have the disadvantage of wasting PMOS transmission.

It also has the effect of lowering the problematic thermal noise by using about twice the existing trans-condensation. For the second stage, the Class-AB structure and the folded-cascode structure for high voltage gain were used to enable low power operation. Finally, for the variability of the voltage of the HEMT drain current, the common mode voltage of the TIA's 1st stage and 2nd stage is also designed to change to four levels through a 2-bit decoder.

### C. Delta-sigma ADC

High resolution ADC is required in the sensor system. If Nyquist-rate ADC is used for high resolution, it is inefficient because of its greater power consumption compared to increased resolution. Therefore, Delta-sigma ADCs can be a good alternative to this [5]. Delta-Sigma ADC can implement high-resolution ADCs without significant power consumption through noise shaping and oversampling techniques. The third order NTF(1) was implemented to implement high resolution ADC [6]. The final digital output value is obtained through the quantification process after a total of three integrations. The block diagram of the proposed structure and the final NTF are as follows. All poles are located in  $(0.5822+j0)$ ,  $(0.934-j0.2792)$ ,  $(0.934+j0.2792)$  and are all present in the original unit so that they do not violate stability. By applying DAC gain, all poles that did not exist in the unit circle were stabilized. In addition, all integration values and DAC gain are optimized for wide dynamic areas and simple signal aggregation processes.

$$NTF = \frac{(1-z^{-1})^3}{1-\frac{49}{20}z^{-1} + \frac{163}{80}z^{-2} - \frac{177}{320}z^{-3}} \quad (1)$$

Ideally, this would give OSR 128 an ENOB equivalent of about 90 dB SQNR, about 15 bits. The output of the TIA (nth value) and the value of the DOUT (N-1th value) through the DAC gain are obtained through the Multi-input comparator through a total of three integral periods. However, despite the use of noise shaping and oversampling, the use of three amplifiers for higher-order shaping results in high waste of power, and delta-sigma ADCs with double sampling structures were used to solve this problem. Unlike traditional sampling methods, by simultaneously implementing sampling and integration processes for each

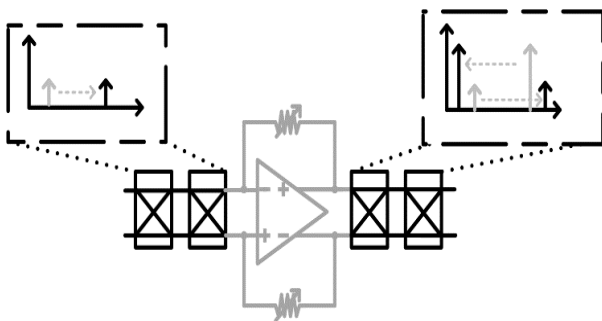


Fig. 6. TIA with chopper Block Diagram.

paper, digital outputs can be obtained to achieve twice the speed [7]. Thus, if the same speed as the existing sampling method is implemented, power consumption can be reduced by about half. To implement this, no additional design complexity is required because it is simply implemented with only a few capacitors and switches. The composition and timing of the ADC using the double sampling technique are shown in Fig. 9 and 10.

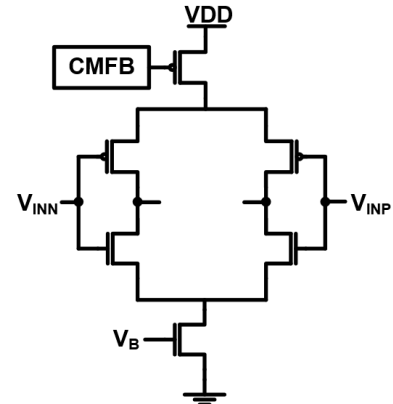


Fig. 7. Complementary Input Amplifier Structure.

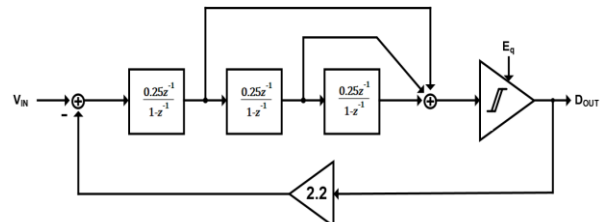


Fig. 8. Third order Noise shaping delta-sigma ADC Block diagram.

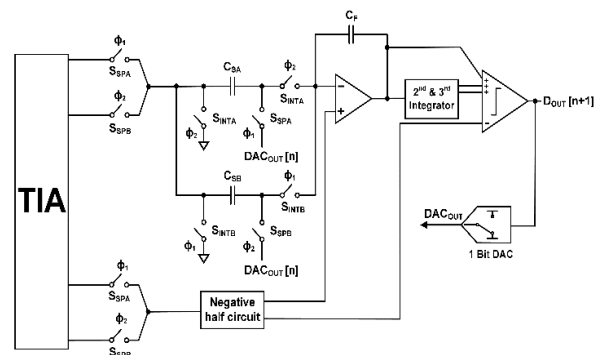


Fig. 9. Delta Sigma ADC with Double Sampling.

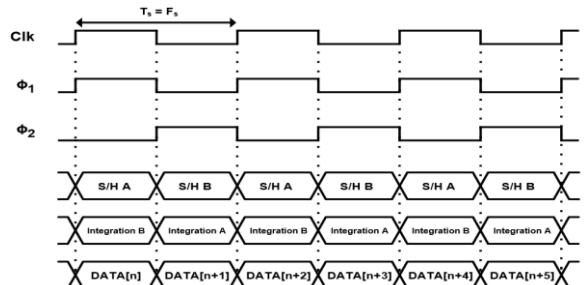


Fig. 10. Delta Sigma ADC Timing with Double Sampling.

The proposed integration structure and common-mode feedback are shown in Fig. 11. Integrator consists of switched-capacitor. Due to problems in power consumption when implementing the Conventional op-amp, the high gain was implemented through inverter-based amplifiers. The inverter-based structure using nmos and pmos can achieve twice as much transconductance as conventional common-source amplifiers and increase the length of input MOS to implement more than 60dB of DC Gain to optimize the performance of ADC. Common-mode feedback is also implemented in switched-capacitor form and is implemented in two sets for double sampling techniques. While one set samples the VCMCMFB, the other set performs a feedback operation to find the correct common-mode output level. After a total of three integration periods, a single-bit quantizer was used instead of Multi-bit quantizer to avoid system complexity. A multi-input comparator performs single-bit quantizer while replacing the role of adding up three integral outputs. The comparator is shown in Fig. 12.

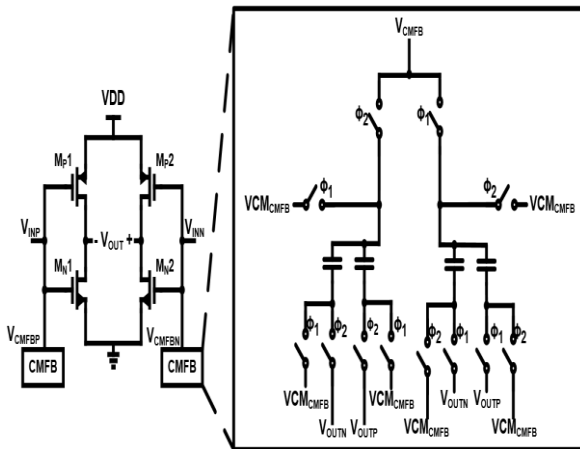


Fig. 11. Delta Sigma ADC with Double Sampling.

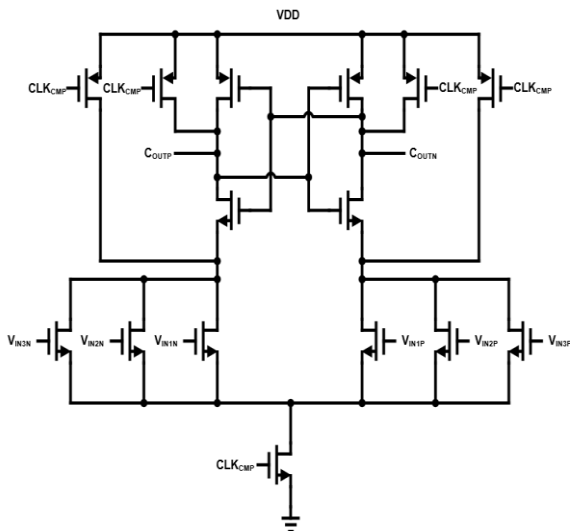


Fig. 12. Delta Sigma ADC with Comparator.

### III. RESULTS

#### A. ADC Result

As shown in Fig. 15, the simulation confirms that it can be approximately 60 dB/decade, i.e. third-order noise shaping. A resolution of approximately 90 dB can be obtained from OSR 128. Therefore, by using an inverter-based amplifier, low power was used and high sensitivity was obtained in a low frequency band.

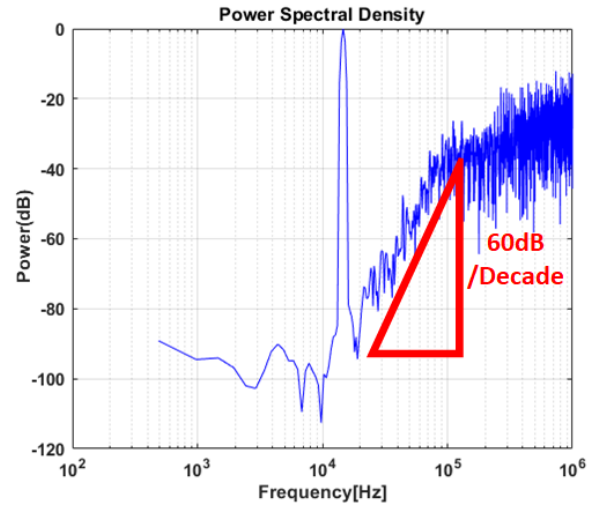


Fig. 15. ADC PSD Plot.

#### B. TIA Result

When the input & output common-mode voltage of TIA is set to 1V and chopping-technique is used and not used, the same plot as Fig.16

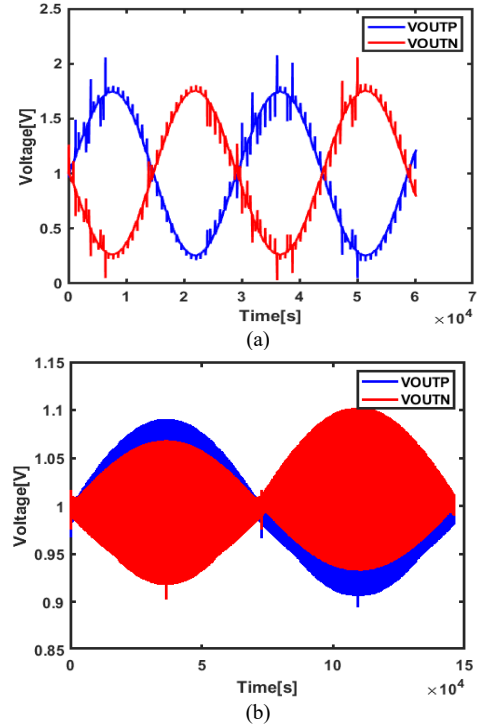


Fig. 16. (a) Chopper on, (b) Chopper off TIA Output.

### C. NCP Result

As shown in Figure 17, it can be seen that the magnitude of the negative voltage, which is an NCP output, changes with the Vref change.

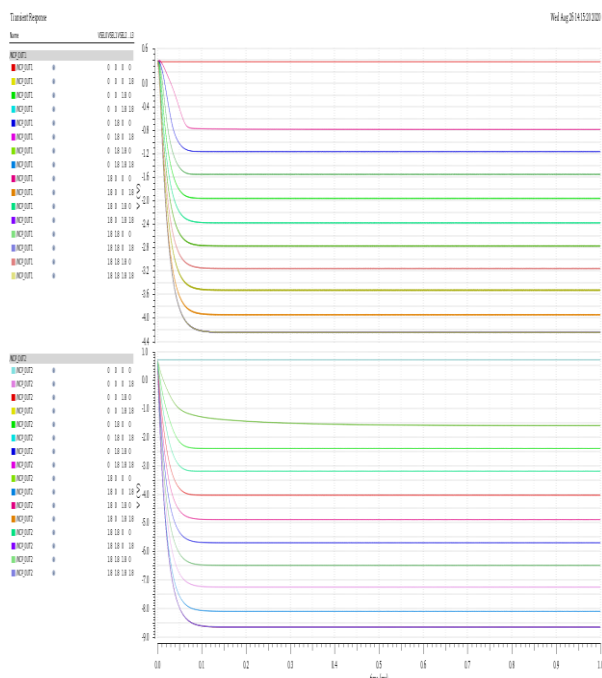


Fig. 17. Negative Charge Pump Output.

### IV. CONCLUSION

In the TSMC 0.18um process, Transimpedance Amplifier (TIA), Delta-Sigma Analog-to-Digital Converter (ADC), and Negative Charge Pump (NCP) were utilized to create low cost, ultra-small, low power, and high-sensitivity sensors.

### ACKNOWLEDGMENT

The chip fabrication and EDA tool were supported by the IC Design Education Center(IDE), Korea.

### REFERENCES

- [1] Ranjan, A.; Agrawal, M.; Radhakrishnan, K.; Dharmarasu, N. Pt/AlGaN/GaN HEMT based ammonia gas sensors. In Proceedings of the IEEE 9th International Nanoelectronics Conferences, Kuching, Malaysia, 3–5 July 2019.
- [2] Ji-Hye Bong, Yong-Jin Kwon, Daejeong Kim, and Kyeong-Sik Min, "Negative charge pump circuit with large output current and high power efficiency," IEICE Electronics Express, 2009, Volume 6, Issue 6, Pages 304-309, Released March 25, 2009.

- [3] Silveira, Fernando & Flandre, Denis & Jespers, P.G.A.(1996). "A gm/ID based methodology for the design of CMOS analog circuits and its application to the synthesis of a silicon-on-insulator micropower OTA. Solid-State Circuits," *IEEE Journal of* 31. 1314 - 1319. 10.1109/4.535416.
- [4] J. F. Witte, K. A. A. Makinwa and J. H. Huijsing, "A CMOS Chopper Offset-Stabilized Opamp," in *IEEE Journal of Solid-State Circuits*, vol. 42, no. 7, pp. 1529-1535, July 2007.
- [5] S. Rabii and B. A. Wooley, "A 1.8-V digital-audio sigma-delta modulator in 0.8- $\mu$ m CMOS," in *IEEE Journal of Solid-State Circuits*, vol. 32, no. 6, pp. 783-796, June 1997.
- [6] J. Roh, S. Byun, Y. Choi, H. Roh, Y. Kim and J. Kwon, "A 0.9-V 60- $\mu$ W 1-Bit Fourth-Order Delta-Sigma Modulator With 83-dB Dynamic Range," in *IEEE Journal of Solid-State Circuits*, vol. 43, no. 2, pp. 361-370, Feb. 2008.
- [7] M. G. Kim et al., "A 0.9 V 92 dB Double-Sampled Switched-RC Delta-Sigma Audio ADC," in *IEEE Journal of Solid-State Circuits*, vol. 43, no. 5, pp. 1195-1206, May 2008.



**Joo Hwan Jin** received the B.S. degrees in electrical engineering from Kookmin University, Seoul, Korea, in 2020. He is currently working toward the M.S. degree in electrical engineering at Konkuk University. His research interests include data converter and IoT sensor.



**Seung Jun Lee** received the B.S. degrees in electrical engineering from Kookmin University, Seoul, Korea, in 2020. He is currently working toward the M.S. degree in electrical engineering at Konkuk University. His research interests include analog to digital converter and IoT sensor.



**Ki Hyun Kim** received the B.S. degrees in electrical engineering from Kookmin University, Seoul, Korea, in 2020. He is currently working toward the M.S. degree in electrical engineering at Konkuk University. His research interests include data converter and IoT sensor.



**Ju Yong Lee** received the B.S. degree in electronic engineering from Kookmin University, Seoul, Korea, in 2020. He is currently working toward the M.S. degree in electrical engineering at Konkuk University. His research during the M.S. course has focused on analog to digital converter, IoT Sensor.



**Hyung Il Chae** received the B.S. degree in electrical engineering from Seoul National University, Seoul, Korea, in 2004, and his M.S. and Ph.D. degrees in electrical engineering from the University of Michigan, Ann Arbor, MI in 2009 and 2013, respectively. From 2013 to 2015, he was a senior engineer at Qualcomm Atheros, San Jose, CA.